Dedicated to my parents

For Their Unwavering Faith, Unmatched Sacrifices and Boundless Support

With Endless Gratitude and Love

DECLARATION

I hereby declare that the thesis entitled "**Characterization, Valorization, and Application of Non-wood Plant-Based Nanocellulose**" submitted to the school of Engineering, Tezpur University, in partial fulfillment of the requirements for the award of the Doctor of Philosophy in the Department of Food Engineering and Technology is a record of original research work carried out by me. Any text, figures, theories, results or designs that are not of my own devising are appropriately referenced in order to give credit to the original author(s). All the sources of assistance have been assigned due acknowledgement. I also declare that neither this work as a whole nor a part of it has been submitted to any other university or institute for any degree, diploma, associateship, fellowship or any other similar title or recognition.

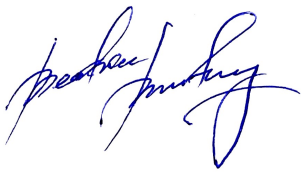

Place: Tezpur (Beatrice Basumatary)

Date: 30-12-2024 Registration Number: TZ189568 of 2018

तेजपुर विश्वविद्यालय/ **TEZPUR UNIVERSITY**
(संसद के अधिनियम द्वारा स्थापित केंद्रीय विश्वविद्यालय)
(A Central University established by an Act of Parliament)
तेजपुर-**784028 :: असम/ TEZPUR-784028 :: ASSAM**

(सर्वोत्तम विश्वविद्यालय के लिए कुलाध्यक्ष पुरस्कार,2016 औरभारत के 100श्रेष्ठ उच्च शिक्षण संस्थानों में पंचम स्थान प्राप्त विश्वविद्यालय)
(Awardee of Visitor's Best University Award, 2016 and 5th among India's Top 100 Universities, MHRD-NIRF Ranking, 2016)

Charu Lata Mahanta
Professor
Department of Food Engineering and Technology
School of Engineering

Email: charu@tezu.ernet.in
Mob: 91-9435092658

CERTIFICATE OF THE SUPERVISOR

This is to certify that the thesis entitled "**Characterization, Valorization and Application of Non-wood Plant-Based Nanocellulose"** submitted to the **School of Engineering, Tezpur University** in partial fulfilment of the requirements for the award of the degree of **Doctor of Philosophy** in the **Department of Food Engineering and Technology** is a record of original research work carried out by **Ms. Beatrice Basumatary** under my supervision and guidance.

All helps received by him from various sources have been duly acknowledged.

No part of this thesis has been submitted elsewhere for the award of any other degree.

Charu Lata Mahanta

Date: 30-12-2024 (Prof. Charu Lata Mahanta)

Place: Tezpur

ACKNOWLEDGEMENT

First and foremost, I thank **Almighty God** for bestowing upon me the strength, courage, wisdom, and perseverance needed to overcome challenges and achieve the successful completion of my research work and thesis.

I express my heartfelt gratitude to all who have supported me throughout this journey. It has been a privilege to work under the guidance of my supervisor, **Prof. Charu Lata Mahanta**. Her academic and personal guidance, coupled with her unwavering support, has been invaluable during my PhD journey. I am deeply indebted to her for her generosity, care, and encouragement, which played a vital role in the successful completion of my thesis. I am especially grateful for her patience and understanding throughout this process. Her knowledge and support have been the foundation upon which I built my achievements.

I would like to express my gratitude to the members of the **Doctoral Committee (DC): Prof. Laximikant S. Badwaik and Prof. Debendra Chandra Baruah** and **Departmental Research Committee (DRC)** for their insightful feedback, guidance, and invaluable contributions that greatly enriched my PhD thesis.

I would like to extend my thanks to the **Head of Department**, **faculty members**, and **technical staff** of the FET department for their selfless service and consideration to me to complete my project.

I am grateful to my **batchmates**, **seniors**, **juniors**, **friends** and all other loving friends and relatives for their love, moral support and encouragement given to me.

I am grateful to the **Ministry of Tribal Affairs (NF-ST)** for granting me a fellowship during my PhD studies.

I appreciate the **Quality Control Lab** and **SAIC** at TU for providing the necessary facilities to conduct and analyze my research.

I would like to express my gratitude to the **Central Library** and **Administration** at Tezpur University.

Finally, my special thanks beyond words go to my **family members** for their deep love, patience and unwavering support.

Here I bow my head before all, as words fail in me to disclose my mind to reveal the flood of gratitude in me.

Ultimately, I offer my heartfelt gratitude to **Almighty God** for His divine intervention, blessings, care, and guidance in every aspect of my life, both past and present, and in all future endeavors.

Beatrice Basumatary

LIST OF TABLES

Table No.	Caption	Page No.
Table 3.1	Independent variables and the coded levels of ultrasonication and High-pressure homogenizer for banana rachis	41
Table 3.2	Independent variables and the coded levels of ultrasonication and High-pressure Homogenizer for pineapple peel	41
Table 3.3	Particle size and zeta potential obtained for the independent variables using ultrasonication	45
Table 3.4	ANOVA of particle size for quadratic model obtained for ultrasonication	46
Table 3.5	ANOVA of zeta potential for quadratic model obtained for ultrasonication	47
Table 3.6	Optimum conditions, experimental and predicted values obtained for ultrasonication	50
Table 3.7	Particle size and zeta potential obtained for the independent variables using high-pressure homogenization	52
Table 3.8	ANOVA of particle size for quadratic model for high-pressure homogenization	53
Table 3.9	ANOVA of zeta potential for quadratic model for high-pressure homogenization	54
Table 3.10	Optimum conditions, experimental and predicted value obtained for high-pressure homogenization	56
Table 3.11	Relative crystallinity and 2θ value of banana rachis, its cellulose fibre and nanocellulose	61
Table 3.12	Thermal parameters of raw and treated banana rachis obtained from DSC analysis	64
Table 3.13	Particle size and zeta potential obtained for the independent variables using ultrasonication	70
Table 3.14	ANOVA of particle size for quadratic model obtained for ultrasonication	71
Table 3.15	ANOVA of zeta potential for quadratic model obtained for ultrasonication	72

Table 3.16	Optimum conditions, experimental and predicted values obtained for ultrasonication	74
Table 3.17	Particle size and zeta potential obtained for the independent variables using ultrasonication	76
Table 3.18	ANOVA of particle size for quadratic model obtained for high-pressure homogenization	77
Table 3.19	ANOVA of zeta potential for quadratic model obtained for high-pressure homogenization	78
Table 3.20	Optimum conditions, experimental and predicted values obtained for high-pressure homogenization	80
Table 3.21	Thermal parameters of raw and treated pineapple peel obtained from DSC analysis	87
Table 3.22	Component content of banana rachis and pineapple peel	91
Table 4.1	Independent variables and their corresponding coded levels	95
Table 4.2	Experimental runs for the development of Pickering nanoemulsion	95
Table 4.3	Different formulation of β-carotene enriched mayonnaise	99
Table 4.4	Responses obtained: Particle size, PDI and Emulsion stability	103
Table 4.5.	ANOVA of particle size for Quadratic model	104
Table 4.6	ANOVA of PDI for Quadratic model	105
Table 4.7	ANOVA of emulsion stability for Quadratic model	106
Table 4.8	Optimum conditions, experimental and predicted values	109
Table 4.9	Colour analysis of functional mayonnaise samples fortified with encapsulated β-carotene over extended storage periods	118
Table 4.10	Texture analysis of functional mayonnaise samples	123
Table 4.11	Power law model parameters of mayonnaise samples	126
Table 4.12	Quantification of identified β-carotene in mayonnaise extract	129
Table 5.1	Formulations of ice cream	139
Table 5.2	The effect of different concentration of banana rachis nanocellulose (BRNC) on texture profile of Double network (DN) hydrogel	147
Table 5.3	Colour parameters of ice cream	153
Table 5.4	Texture parameters of ice cream	154

Table 6.1	Formulations used to develop aerogels and bioactive aerogels	169
Table 6.2	Relative crystallinity and 2θ values of control and bioactive aerogels	180
Table 6.3	Density and porosity of control and bioactive aerogels	183
Table 6.4	Colour change of indicator and TVB-N (mg/100 g of meat), pH changes and TVC (log_{10}CFU/g) in minced meat during storage	190

LIST OF FIGURE

Figure No.	Caption	Page No.
Fig. 2.1	Formation of Pickering emulsion.	16
Fig. 2.2	Diagrammatic representation of (a) the addition of CNF after the emulsification process (b) three stabilisation regimes are displayed (c) depletion flocculation of oil droplets in the CNC-stabilized Pickering emulsions.	18
Fig. 3.1	Sequence of steps followed for nanocellulose isolation.	44
Fig. 3.2	Stages of treatment during nanocellulose isolation from banana rachis.	44
Fig. 3.3	3D surface graphs of (a, b) particle size and (c, d) zeta potential of nanocellulose obtained by ultrasonication.	49
Fig. 3.4	Particle size distribution and zeta potential of the nanocellulose obtained by ultrasonication.	51
Fig. 3.5	3D surface graphs of (a, b) particle size and (c, d) zeta potential of nanocellulose obtained by high-pressure homogenization.	55
Fig. 3.6	Particle size distribution and zeta potential of the nanocellulose obtained by high pressure homogenization.	57
Fig. 3.7	(a) Images of nanocellulose suspension obtained from banana rachis, (b) Freeze dried nanocellulose, (c) SEM images of cellulose obtained from ultrasonication and (d) SEM images of cellulose obtained from high pressure homogenization.	59
Fig. 3.8	FTIR spectra of powdered banana rachis (BR), cellulose fibre (CF) and nanocellulose (NC) of ultrasonicated samples.	60
Fig. 3.9	Overlaid powdered X-ray diffraction of ultrasonicated samples. BR, banana rachis; CF, cellulose fibre; and NC, nanocellulose.	61
Fig. 3.10	TGA, and DTG curve of samples. BR, banana rachis; CF, cellulose fibre; and NC, nanocellulose.	62
Fig. 3.11	DSC curve of (a) banana rachis powder, (b) cellulose fibre, and (c) nanocellulose.	65
Fig. 3.12	FE-SEM micrographs of the BR, CF, and NC for 10 μm (a, b, and c) and 1 μm (x, y, and z) scale, respectively.	66

Fig. 3.13	TEM micrograph of the nanocellulose (NC).	67
Fig. 3.14	AFM image of the nanocellulose.	68
Fig. 3.15	Stages of treatment during nanocellulose isolation from pineapple peel.	69
Fig. 3.16	3D surface graphs of (a, b) particle size and (c, d) zeta potential of nanocellulose obtained by ultrasonication.	73
Fig. 3.17	Particle size distribution and zeta potential of the nanocellulose obtained by ultrasonication.	75
Fig. 3.18	3D surface graphs of (a, b) particle size and (c, d) zeta potential of nanocellulose obtained by high-pressure homogenization.	79
Fig. 3.19	Particle size and zeta potential of the nanocellulose obtained by high-pressure homogenization.	81
Fig. 3.20	(a) Images of cellulose, (b) nanocellulose obtained from pineapple peel, (c) SEM images of nanocellulose obtained from ultrasonication and (d) SEM images of nanocellulose obtained from high pressure homogenization.	83
Fig. 3.21	FTIR spectra of powdered pineapple peel (PP), cellulose fibre (CF) and nanocellulose (NC).	84
Fig. 3.22	X- ray diffraction of powdered pineapple peel (PP), cellulose fibre (CF) and nanocellulose (NC).	85
Fig. 3.23.	Thermogravimetric analysis and 1ST derivatives (DTG) of pineapple peel (PP), cellulose fibre (CF) and nanocellulose (NC).	86
Fig. 3.24	DSC curve of raw (a) pineapple peel powder, (b) cellulose fibre and (c) nanocellulose.	88
Fig. 3.25	TEM micrograph of the nanocellulose (NC).	89
Fig. 3.26	AFM image of the nanocellulose (NC).	90
Fig. 4.1	3D surface graphs: (a, b) particle size, (c, d) PDI, and (e-f) emulsion stability.	108
Fig. 4.2	Particle size analysis of optimized Pickering nanoemulsion.	110
Fig. 4.3	Physical stability check of optimized emulsion during storage at 25°C for 35 days.	111

Fig. 4.4	Particle size of optimized Pickering emulsion for a period of 35 days.	112
Fig. 4.5	Optical microscopy images of Pickering nanoemulsion (PNE) stabilized with nanocellulose in optimized processing parameters obtained at 7 days interval during storage at RT (28°C) for 35 days.	115
Fig. 4.6	Degradation curve of β-carotene in ethanol solution (control) and in PNEs under UV-light (C is the content of β-carotene after storage for a period t against UV light, while C_0 is the initial β-carotene content at preparation of stabilized β-carotene-loaded Pickering emulsions).	116
Fig. 4.7	Appearance of functional mayonnaise enriched with Pickering nanoemulsions loaded with β-carotene.	119
Fig. 4.8	Optical microscopic images of mayonnaise enriched with Pickering nanoemulsions loaded with β-carotene.	121
Fig. 4.9	Amount of hydroperoxides in mayonnaise samples fortified with β-carotene during 14 days of storage at 4°C.	124
Fig. 4.10	(a): Storage modulus (G') and (b): loss modulus (G”) values (in log) against angular frequency of mayonnaise products enriched with Pickering nanoemulsions loaded with β-carotene.	125
Fig. 4.11	HPLC chromatograms of β-carotene present in mayonnaise samples.	128
Fig. 4.12	Intestinal lipolysis profile of the mayonnaise samples stabilized by Pickering nanoemulsions.	130
Fig. 4.13	β-carotene bioaccessibility of mayonnaise samples after in-vitro digestion.	131
Fig. 5.1	Appearance of DN hydrogels loaded with different concentration of banana rachis nanocellulose (BRNC).	143
Fig. 5.2	Thermogravimetric analysis and 1^{ST} derivatives (DTG) of DN hydrogels with different concentration of BRNC.	145
Fig. 5.3	Water holding capacity (WHC) of DN hydrogels with different concentration of BRNC.	149

Fig. 5.4	Dynamic rheological properties of hydrogels at different concentration of banana rachis nanocellulose (BRNC). (A) Storage modulus G′, (B) loss modulus G″, and (C) tan δ during the heating process, (D) Storage modulus G′, (E) loss modulus G″, and (F) tan δ during the cooling process.	151
Fig. 5.5	Images of ice creams incorporated with β-carotene-enriched hydrogels.	152
Fig. 5.6	Overrun, gas-hold up, and meltdown of ice creams. Different letters indicate significant differences between samples at $p < 0.05$.	156
Fig. 5.7	(A) Shear stress, (B) Apparent viscosity, (C) Storage modulus (G'), (D) Loss modulus (G"), and (E) Tan δ of ice creams.	159
Fig. 5.8	Free fatty acids release during digestion of ice cream.	161
Fig. 5.9	Bioaccessibility of β-carotene in ice creams.	162
Fig. 6.1	Image of the (a) raw butterfly pea flower (b) Freeze dried, and (c) Powder form of flower.	173
Fig. 6.2	Chromatogram of the butterfly pea flower extract detected at 330 nm. Peak 1, Delphinidin-3-rutinoside; peak 2, Cynadin-3-rutinoside; and peak 3, Pelargonidin-3-rutinoside.	174
Fig. 6.3	Chromatogram of the butterfly pea flower extract detected at 330 nm. Peak no. 1,2,3, not yet identified; 4: Gallic acid; 5: Chlorogenic acid; 6: Caffeic acid; 7: *p*-Coumaric acid.	175
Fig. 6.4	Image of aerogels prepared with (a) PVA, (b) PVA/CF, (c) PVA/CF/NC, (d) PVA/BPFE, (e) PVA/CF/BPFE, and (f) PVA/CF/NC/BPFE before freeze drying.	176
Fig. 6.5	Morphology of aerogels made with (a) PVA, (b) PVA+CF, (c) PVA+CF+NC, (d) PVA+BPFE, (e) PVA+CF+BPFE, and (f) PVA+CF+NC+BPFE. PVA: polyvinyl alcohol; CF: cellulose fibre; NC: nanocellulose; BPFE: Butterfly pea flower extract.	177
Fig. 6.6	(a) FT-IR spectra of the bioactive and non-bioactive aerogels, (b) expansion of the zone between 1800 cm^{-1} and 600 cm^{-1}.	179
Fig. 6.7	Overlaid powdered XRD pattern of aerogels with and without BPFE. BPFE: butterfly pea flower extract.	181

Fig. 6.8	(a) Thermal analysis (TGA), and (b) its first derivatives (DTG) of the aerogels with and without BPFE. BPFE: butterfly pea flower extract.	182
Fig. 6.9	Water absorption by aerogels made of PVA, PVA+CF, and PVA+CF+NC.	184
Fig. 6.10	BPFE's and a bioactive aerogels' antioxidant properties. The data here at are presented as the mean (n=3), and the standard deviation is shown by the bars in the columns. Significant differences between values in a column for each letter ($p<0.05$).	185
Fig. 6.11	In-vitro release of BPFE from aerogels under (a) hydrophilic and (b) hydrophobic food simulation conditions.	187
Fig. 6.12	Colour change response of butterfly pea flower (BPF) solution and BPF based aerogels at pH 3, 5, 7, 9 and 10.	188
Fig. 6.13	(A) Reversibility of the BPF-based aerogels to ammonia and acetic acid vapours and (B) Apparent colour change of BPF-based aerogel in minced meat during storage at 4°C.	189

LIST OF ABBREVIATIONS

Abbreviations	Full Form
ENM	Engineered Nanomaterial
BC	Bacterial Nanocellulose
BR	Banana Rachis
PP	Pineapple Peel
CF	Cellulose Fibre
CNCs	Cellulose Nanocrystals
CNFs	Cellulose Nanofibrils
NC	Nanocellulose
PNE	Pickering Nanoemulsions
BRNC	Banana Rachis Nanocellulose
HPH	High-Pressure Homogenisation
XRD	X-Ray Diffraction
TEM	Transmission Electron Microscopy
FESEM	Field Emission Scanning Electron Microscopy
SEM	Scanning Electron Microscopy
AFM	Atomic Force Microscopy
UV-Vis	UV-Visible Spectroscopy
FTIR	Fourier-Transform Infrared Spectroscopy
TGA	Thermogravimetric Analysis
DSC	Differential Scanning Calorimetry
DLS	Dynamic Light Scattering
GIT	Gastrointestinal System
NEs	Nanoemulsions
PUFAs	Polyunsaturated Fatty Acids
SPI	Soy Protein Isolate
DTG	Derivative Thermogravimetric
ANOVA	Analysis Of Variance
US	Ultrasonication
PDI	Poly dispersibility Index
BBD	Box-Behnken Design

RSM	Response Surface Methodology
RP-HPLC	Reverse Phase- High Performance Liquid Chromatography
SGF	Simulated Gastric Fluid
SIF	Simulated Intestinal Fluid
DN	Double Network
WHC	Water Holding Capacity
TVB-N	Total Volatile Bases-Nitrogen
BPFE	Butterfly Pea Flower Extract
PVA	Polyvinyl Alcohol
TVC	Total Viable Count

LIST OF SYMBOLS

Symbols	Full form
Aa	Amorphous Region
Ac	Crystalline Region
nm	Nanometer
mg	Milligram
°C	Degree Celsius
g	Grams
h	Hours
Kg	Kilograms
KOH	Potassium Hydroxide
L	Litre
mL	Milli litre
m	Mass
min	Minutes
sec	Seconds
t	Time
T	Temperature
V	Volume
W	Watt
μg	Micro Gram (10^{-6}kg)
To	Onset Temperature
Tp	Peak Temperature
Tc	Conclusion Temperature
ΔH	Enthalpy
kV	Kilo Volt
cu	Copper
mV	Milli Volt
%	Percentage
Z	Coded Levels
Z_0	Actual Levels
ΔZ	Step Change
Z_c	Actual Value at Central Point

R^2	Determination Coefficient
cm^{-1}	Per Centimetre
θ	Theta
J/g	Joule Per Gram
b*	Yellowness
a*	Redness
L*	Lightness
V_{NaOH}	Volume of NaoH
C_{NaOH}	Concentration of NaoH
M	Molecular Weight of Oil
rpm	Revolutions Per Minute
RT	Room Temperature
C	Content Of B-Carotene After Storage
C_0	Initial B-Carotene Content
G'	Storage Modulus
G''	Loss Modulus
K	Consistency Index
n	Flow Behaviour Index
W_b	Weight of the Centrifuge Tube Before Centrifugation
W_c	Weight of the Empty Centrifuge Tube
W_a	Weight ff the Centrifuge Tube After Blotting off the Residual Water
tan δ	Phase Angle
Pa	Pascal
ΔE	Overall Colour Difference
g.s	Gram Sec
W_d	Weight of the Dried Sample
W_s	Weight of the Swollen Aerogels
W_a	Aerogels' Weight in Grams
ρc	Density of Cellulose
ABS	Absorbance